Supplementary Information

Procedure for noise cross-correlation computation and stacking

Figure S1 synthesizes the cross-correlation procedure. To normalize the seismic noise in time and spectral domains, we applied a spectral whitening followed by a one-bit normalization. For spectral whitening, we take the seismic signal Fourier transform and normalize its modulus to one in the selected frequency band and force its modulus to 0 elsewhere (smoothed boxcar window). We do not change the phase of the Fourier transform. We finally perform an inverse Fourier transform to retrieve the whitened signal. By doing so, we do not change the spectral phase of the signal. We also computed the RTP using a different normalisation when the running-absolute-mean normalization in time domain was followed by the spectral whitening[1]. Results of this test shown in Fig. S2 demonstrate that the RTP anomalies computed with different data processing methods are very similar to each other. Finally, we prefer to use the one-bit normalization because it is faster than the running-absolute-mean normalization and better removes strong glitches from the signal. In this study, we compute the reference Green functions by stacking the one-day cross-correlation functions (CCF) according to a signal to noise ratio criterion (CCF signal energy larger than 1.5 times the CCF noise energy, 411 over 550 one-day CCF stacked on average).

Procedure for measuring Relative Time Perturbations (RTP)

We remind that the cross-correlation of seismic noise between receivers A and B yields the Green functions between A and B (positive times, causal) and between B and A (negative times, anti-causal). In case of perfect reconstruction, these two Green functions are identical. In Fig. S3a, we schematically illustrate possible paths for the reconstructed diffracted surface waves. We now consider a uniform relative shear wave velocity decrease within the sampled medium ($\Delta\beta/\beta$ = const.). In this case, scattered waves that travelled along longer paths accumulated larger time delays ($\Delta\tau$). The Green function estimated after the velocity change (red signal) will, therefore, correspond to a

stretched version of the reference function (Fig. S3b). We then consider a small window of width T and centred on time τ. We compute a cross-spectrum between the reference and current Green functions taken within this small window and measure the spectral phase shift Φ at different frequencies f (Fig. S3c). For each frequency, the phase error E_Φ is estimated by:

$$E_\Phi = \frac{1}{2 \times B_\omega \times T} \times (1/c^2 - 1),$$

where c is the coherency and B_ω is the spectral width. The local time shift between the current and the reference Green functions is then estimated as the slope b = Δτ = Φ/(2 × π × f) by a linear regression that takes into account the phase error E_Φ as a weighting factor. The error on the slope estimate (Δτ) is calculated as:

$$E_{\Delta\tau} = \frac{\sigma_\Phi}{\sum_{i=1}^{M} (f_i - \bar{f})^2} \quad \text{with} \quad \sigma_\Phi = \frac{\sum_{i=1}^{M} (\Phi_i - \bar{\Phi})^2}{M}, \quad \bar{\Phi} = 2\pi \times \Delta\tau \times f_i,$$

where M is the number of frequency samples and $\bar{f}$, the average frequency. By repeating this operation for a series of small windows centred at different times we estimate the local time shift as a function of time: Δτ (τ). In a case of a uniform velocity perturbation within the media it is expected to be a linear function (Fig. S3d). Therefore, we measure the slope of the travel time shifts along the estimated Green functions (for positive and negative times, Fig. S3d) to estimate the Relative Time Perturbation (RTP) that the opposite of the medium's uniform relative shear wave velocity variation. The error on the RTP estimate (Δτ/τ) is calculated as:

$$E_{\Delta\tau/\tau} = \frac{\sigma_{\Delta\tau}}{\sum_{i=1}^{M} (\tau_i)^2} \quad \text{with} \quad \sigma_{\Delta\tau} = \frac{\sum_{i=1}^{M} (\Delta\tau_i - \Delta\bar{\tau})^2}{N}, \quad \Delta\bar{\tau} = \Delta\tau/\tau \times \tau_i,$$

where N is the number of time samples. We emphasize that only a physical velocity variation of the sampled medium can explain the symmetry in the time shifts along the coda of the positive and negative time cross-correlation functions[2]. Moreover, measuring the time shift linear trend by linear regression (LSQR) passing through 0 allows us to bypass the artefacts of instrumental errors. This makes our approach robust and allows us to measure relative velocity variations smaller than 0.1%.

Length of the moving window

We use 10-days-long moving windows to compute "current" noise cross correlations. This value was selected as a trade-off between time resolution and stability of the Green function reconstruction. Our tests showed that using shorter moving windows deteriorates in stability of reconstruction increasing the noise level of the RTP measurements. This is illustrated with Fig. S4a that shows the RTP measured using "current" cross-correlations computed from five-days-long moving windows. In this case, amplitudes of pre-eruptive anomalies are slightly increased while the level of the measurement noise is increased significantly. At the same time, it can be seen that the length of the moving window does not affect significantly the precursors duration. We also tested measurements using one-day moving windows. In this case, the RTP noise level becomes too strong and only the strongest precursor (before eruption 4) can be distinguished.

Regionalization method

We localize the relative velocity changes in space by applying a regionalization procedure. We measure the Relative Time Perturbations (RTP) for each receiver pair separately. The LTV (Long Term Variation) is obtained by estimation of the 11 order polynomial fit to the relative velocity changes. The periodicity of the LTV is about 6 months. The STV (Short Term Variation) is obtained by subtracting the LTV from the relative velocity changes (Fig. S5a). We distribute, for each receiver pair, for each day,

and for the STV and LTV separately, the values of $\Delta v/v$ ($= -\Delta\tau/\tau$) within grid cells which distances to the direct paths are smaller than 2 km (Fig. S5b). We then average, for every grid cell, their associated values of $\Delta v/v$. In case of denser receiver networks, it would be worth optimizing this procedure by taking into account more realistic sensitivity kernels of the coda time shifts for localized velocity perturbations[3].

Long Term Variations (LTV)

The analysis of the long-term velocity variations (LTV) shows that they are related to processes varying over several months with a possible seasonality (Figs. S2b and S4a). A clear seasonal dependence of the seismic velocity changes was observed from the analysis of short-period noise cross-correlations at the Merapi volcano[4] and was related to variations of the depth of the superficial ground water layer because of precipitation. In the case of the Piton de la Fournaise, the observed LTV can not be only related to the precipitations on *La Réunion* island (Figs S4a and S4c). Moreover, the LTV amplitude and location (east of Dolomieu crater) are very similar to what was observed for the short-term precursors (Figs. S5d and S5e) suggesting that the long-term velocity variations reported in this study are likely to be partly related to the dynamics of the volcano-magmatic system.

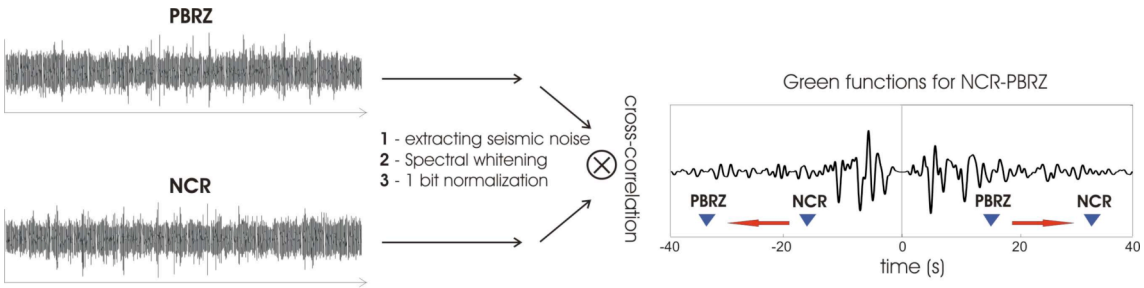

Supplementary Figure 1: The Green function reconstruction procedure. The presented Green function is filtered ([0.1-0.9] Hz). The positive and negative time Green functions are normalized separately to highlight the phase symmetry.

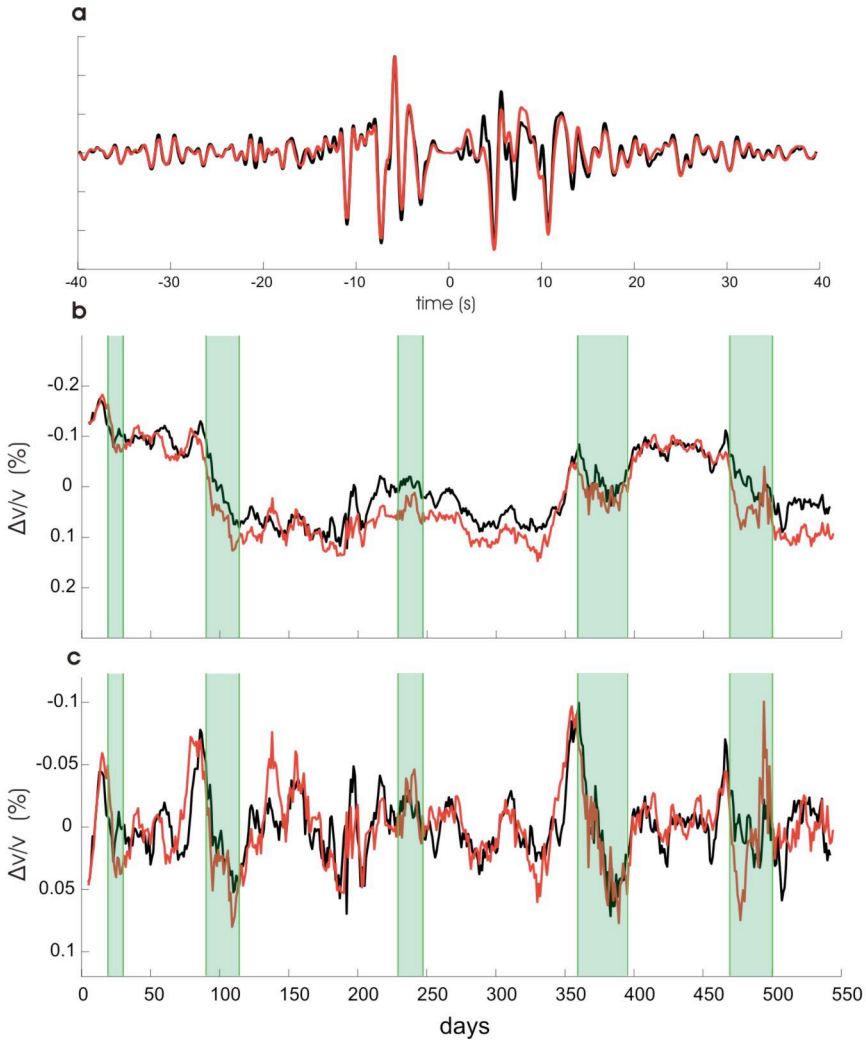

Supplementary Figure 2: Comparison of the RTP measurements obtained with different data processing methods. The black curves are obtained from cross-correlations computed with spectral whitening followed by one-bit normalization. The red curves are obtained from cross-correlations computed with running-absolute-mean normalization followed by spectral whitening. **(a)** Filtered ([0.1-0.9] Hz) reference cross-correlation functions (receiver pair PBRZ-NCR). The positive and negative time Green functions are normalized separately to highlight the phase symmetry.
(b) Raw Relative Time Perturbations **(c)** Relative Time Perturbations corrected from the Long Term Variations.

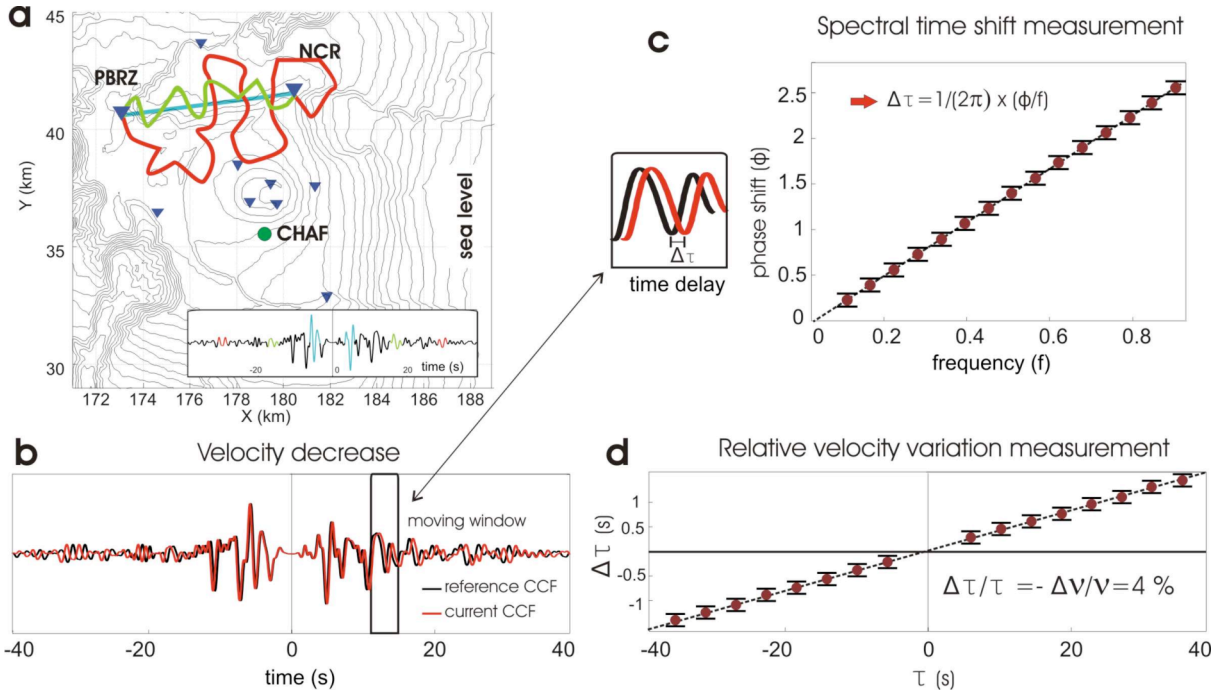

Supplementary Figure 3: Synthetic case illustrating the procedure of the RTP measurement. **(a)** Possible paths for the reconstructed diffracted Rayleigh waves. The green circle corresponds to the extensometer location. **(b)** The black signal is the reference Green function for receiver pair PBRZ-NCR ([0.1-0.9] Hz). The red signal is the synthetic current Green function corresponding to a uniform 4 % relative velocity decrease within the volcano edifice. The positive and negative time Green functions are normalized separately to highlight the phase symmetry. **(c)** Time shift estimation from the linear regression of the cross-spectrum phase. **(d)** Measured time shifts between the reference and the perturbed Green functions and a corresponding RTP measurement ($\Delta\tau/\tau$).

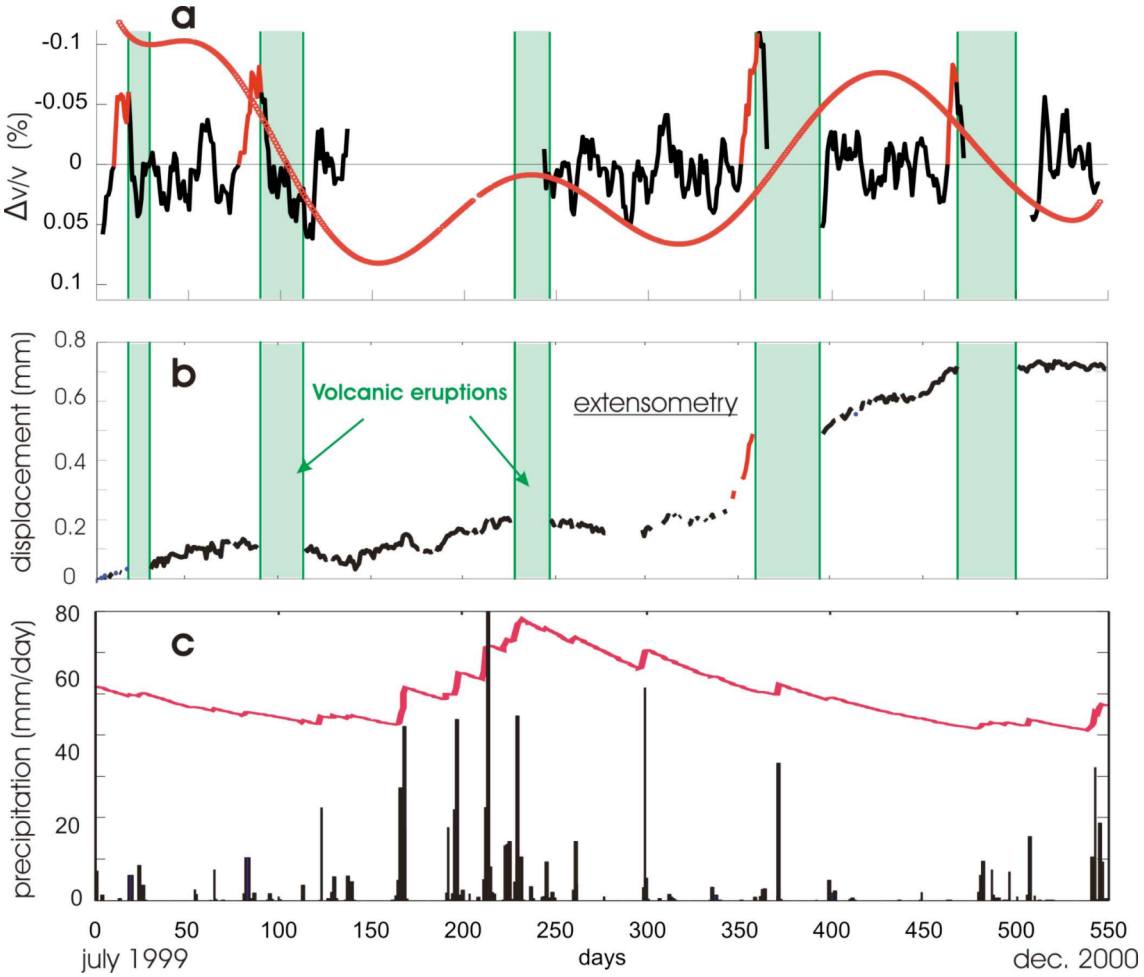

Supplementary Figure 4: **(a)** Relative velocity changes calculated computed using five-days-long moving windows. The STV and LTV are respectively represented by black and red curves. **(b)** Extensometer (CHAF) data (see Fig. S3a). **(c)** Pluviometry provided by the NASA/Goddard Space Flight Center's Laboratory for Atmospheres[5]. Realistic precipitation values for the Piton de la Fournaise volcano are approximatively five times greater. We use a hydrological model[4] to qualitatively describe the temporal evolution of the water table height (red curve).

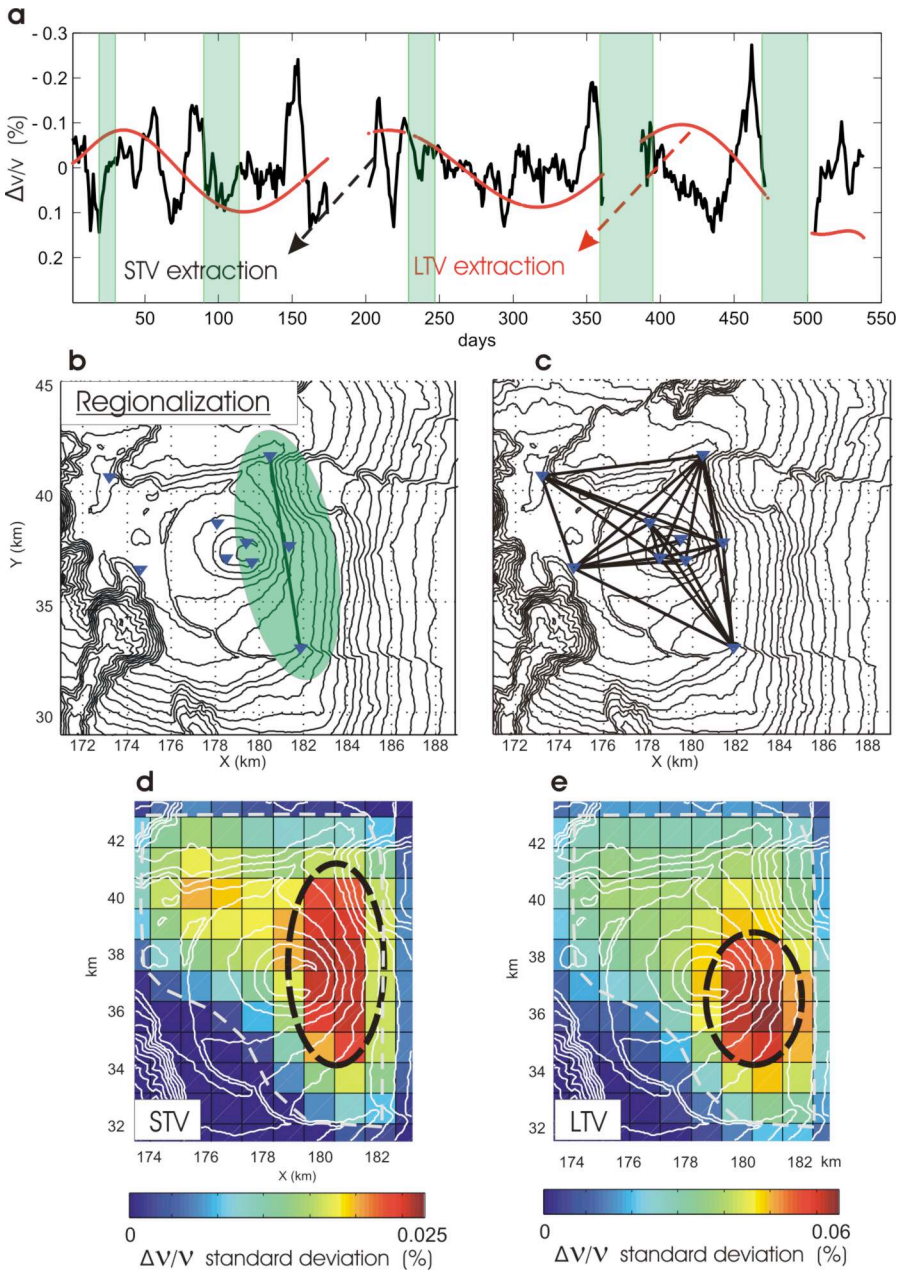

Supplementary Figure 5: **(a)** Extraction of the short- and long-term variations for receiver pair NTR-NCR. **(b)** A sensitivity zone corresponding to measured relative perturbations. **(c)** Topographic map showing the receiver pairs used for the regionalization procedure. **(d)** Standard deviation of the regionalized short-term negative relative velocity changes. The gray dashed line represents the limits of ray coverage. **(e)** Standard deviation of the regionalized long-term relative velocity changes.

References

1. Bensen, G.D., M.H. Ritzwoller, M.P. Barmin, A.L. Levshin, F. Lin, M.P. Moschetti, N.M. Shapiro, and Y. Yang, Processing seismic ambient noise data to obtain reliable broad-band surface wave dispersion measurements, *Geophys. J. Int.*, 169, 1239–1260, doi:10.1111/j.1365-246X.2007.03374.x (2007).

2. L. Stehly, M. Campillo, N. M. Shapiro, Travel time measurements from noise correlation: stability and detection of instrumental errors, *Geophys. J. Int.* doi:10.1111/j.1365-246X.2007.03492.x (2007).

3. C. Pacheco, R. Snieder, Time-lapse traveltime change of singly scattered acoustic waves, *Geophys. J. Int.* **165**, 485 (2006).

4. C. Sens-Schönfelder, U. Wegler, Passive image interferometry and seasonal variations of seismic velocities at Merapi Volcano, Indonesia, *Geophys. Res. Lett.* **33** (2006).

5. G. Huffman, et al., Global precipitation at one-degree daily resolution from multi-satellite observations, *J. Hydrometeorol.* **2**, 36 (2001).